

Optical properties of La-based high- K dielectric films

E. Cicerella, J. L. Freeouf, L. F. Edge, D. G. Schlom, T. Heeg, J. Schubert, and S. A. Chambers

Citation: *Journal of Vacuum Science & Technology A* **23**, 1676 (2005); doi: 10.1116/1.2056555

View online: <http://dx.doi.org/10.1116/1.2056555>

View Table of Contents: <http://scitation.aip.org/content/avs/journal/jvsta/23/6?ver=pdfcov>

Published by the AVS: Science & Technology of Materials, Interfaces, and Processing

Articles you may be interested in

[Solution processed lanthanum aluminate gate dielectrics for use in metal oxide-based thin film transistors](#)
Appl. Phys. Lett. **106**, 203507 (2015); 10.1063/1.4921262

[Optical band gaps and composition dependence of hafnium–aluminate thin films grown by atomic layer chemical vapor deposition](#)
J. Vac. Sci. Technol. A **23**, 1706 (2005); 10.1116/1.2091096

[Optical and electrical properties of amorphous Gd x Ga 0.4–x O 0.6 films in Gd x Ga 0.4–x O 0.6 / Ga 2 O 3 gate dielectric stacks on GaAs](#)
Appl. Phys. Lett. **84**, 2521 (2004); 10.1063/1.1695445

[Growth and physical properties of Ga 2 O 3 thin films on GaAs\(001\) substrate by molecular-beam epitaxy](#)
Appl. Phys. Lett. **82**, 2978 (2003); 10.1063/1.1572478

[Spectroscopic ellipsometry characterization of high-k dielectric HfO 2 thin films and the high-temperature annealing effects on their optical properties](#)
Appl. Phys. Lett. **80**, 1249 (2002); 10.1063/1.1448384

ADVERTISEMENT

Instruments for advanced science

Gas Analysis



- dynamic measurement of reaction gas streams
- catalysis and thermal analysis
- molecular beam studies
- dissolved species probes
- fermentation, environmental and ecological studies

Surface Science



- UHV TPD
- SIMS
- end point detection in ion beam etch
- elemental imaging - surface mapping

Plasma Diagnostics



- plasma source characterization
- etch and deposition process reaction kinetic studies
- analysis of neutral and radical species

Vacuum Analysis



- partial pressure measurement and control of process gases
- reactive sputter process control
- vacuum diagnostics
- vacuum coating process monitoring

contact Hiden Analytical for further details



info@hideninc.com
www.HidenAnalytical.com
CLICK to view our product catalogue 

Optical properties of La-based high-*K* dielectric films

E. Cicerella^{a)} and J. L. Freeouf^{b)}

Department of Electrical and Computer Engineering, Oregon Health and Sciences University, Beaverton, Oregon 97006

L. F. Edge and D. G. Schlom

Department of Materials Science and Engineering, The Pennsylvania State University, University Park, Pennsylvania 16802

T. Heeg and J. Schubert

Institut für Schichten und Grenzflächen, ISG 1-IT, and CNI, Forschungszentrum Jülich GmbH, 52425 Jülich, Germany

S. A. Chambers

Fundamental Science Directorate, Pacific Northwest National Laboratory, Richland, Washington 99352

(Received 16 November 2004; accepted 8 August 2005; published 25 October 2005)

We have characterized thin films of LaScO₃ and LaAlO₃ which were grown by molecular beam deposition on Si substrates. Samples of LaScO₃ were also grown by pulsed laser deposition on MgO substrates. Using transmission studies between 1.5 and 6 eV, we have established that low temperature deposition leads to a reduced band gap with respect to the bulk crystal. Furthermore, using spectroscopic ellipsometry from 5 to 9 eV we observe substantial differences in near-band gap absorption between thin and thicker films for both materials. We obtain a band gap of 5.84 eV for the thinner film of LaAlO₃, whereas we find a band gap of 6.33 eV for the thicker film of LaAlO₃. Similarly we find band gaps of 5.5 and 5.96 eV, respectively, for thin and thick films of LaScO₃. © 2005 American Vacuum Society. [DOI: 10.1116/1.2056555]

I. INTRODUCTION

As SiO₂ approaches its limits as an effective gate dielectric in metal-oxide-semiconductor field-effect transistors,^{1–5} there is a wide range of research being conducted on alternative materials.^{6–12} Replacement materials must have a high dielectric constant, must be thermally stable with Si, have a large band gap, and have at least one 1 eV band offsets with Si for both holes and electrons.^{13–18} We have found some rare earth perovskites that may offer the desired properties.^{19–22} These materials have high dielectric constants,^{23,24} and we expect them to be thermodynamically stable with silicon.²⁵ In this work thin films of two contending materials, LaScO₃ and LaAlO₃, were grown by molecular beam deposition (MBD) on Si substrates. Also, thin films of LaScO₃ were grown by pulsed laser deposition (PLD) on MgO substrates. We studied these materials using spectroscopic ellipsometry in the far ultraviolet (UV) (5–9 eV) and the UV/visible (1.5–5 eV), as well as transmission studies between 1.5 and 6 eV.

II. EXPERIMENT

Films of LaScO₃ were deposited by MBD on Si (100) substrate. The amorphous LaScO₃ films were grown by MBD in an EPI 930 molecular-beam epitaxy chamber modified for the growth of oxides.²⁶ The films were grown on *n*- and *p*-type Si (001) wafers. The native SiO₂ on the silicon

wafer was thermally removed in ultrahigh-vacuum (UHV) at a temperature of 900 °C, measured with an optical pyrometer. Two films had nominal thicknesses of 30 and 100 nm. The thicknesses were determined by calibrating the fluxes using a quartz crystal microbalance and assuming the films had the bulk density of single crystal LaScO₃.

Also studied were epitaxial and amorphous films of LaScO₃ grown by PLD, using a KrF excimer laser (wavelength 248 nm, pulse width 20 ns, and a fluence of 2.5 J/cm²).²⁷ Rotating cylindrical targets, made from sintered powder of stoichiometric composition, have been used as starting materials.²⁸ For the on-axis geometry, the substrate is placed into the center of the PLD plasma plume. This allows a high deposition rate with a limited area of uniformity (in this case 1 × 1 cm²). The substrates are positioned directly onto a SiC resistive heater and an oxygen gas partial pressure of 2 × 10⁻³ mbar is maintained during the deposition process.²⁹ The epitaxial and amorphous films of LaScO₃ were grown in this on-axis geometry onto MgO(100) 1 × 1 cm² substrates with a 10 nm thin BaTiO₃ interlayer (necessary for epitaxial growth on MgO) also grown with PLD. For the epitaxial LaScO₃ sample on MgO, a substrate temperature of 750 °C was used.

The amorphous LaAlO₃ films were grown by MBD in an EPI 930 molecular-beam epitaxy chamber modified for the growth of oxides. The films were grown on *n*- and *p*-type Si (001) wafers. The native SiO₂ on the silicon wafer was thermally removed in UHV at a temperature of 900 °C, measured with an optical pyrometer. The films were grown using elemental sources. Lanthanum, aluminum, and molecular oxygen (99.994% purity) at a background pressure of 6

^{a)}Present address: Department of Physics, Portland State University, P.O. Box 751, Portland, OR 97207-0751.

^{b)}Author to whom correspondence should be addressed; electronic mail: jfreeouf@pdx.edu

TABLE I. Results of Sellmeier fit to two films of LaScO₃/Si.

Film	Thickness (nm)	A_n	B_n	C_n (nm)
Thin	39.6±0.2	3.42	0.32	245.58
Thick	141.3±2	3.26	0.48	229.76

× 10⁻⁸ Torr were codeposited at a thermocouple temperature of ~100 °C onto the clean 2 × 1 Si surface. The lanthanum and aluminum fluxes were each 2 × 10¹³ atoms/cm² s.³⁰ As with the LaScO₃, the thicknesses of the LaAlO₃ films were calibrated assuming the films had the density of bulk single crystal material, in this case, single crystal LaAlO₃.

Ellipsometry data from the samples were measured in two systems. One was a commercial system, the Rudolph S2000, and the other was a custom-fabricated system. The Rudolph system uses a fixed polarizer-rotating polarizer-sample-(compensator)-fixed polarizer approach and has a nominal range of 250–850 nm.

For higher photon energy measurements we used a custom-fabricated system, which was installed in a glove box under nitrogen ambient. This is a conventional fixed polarizer-sample-rotating polarizer design. It uses far UV optical components, including MgF₂ Rochon prisms, and a sodium salicylate coating to permit high energy photon detection with a conventional quartz-window photomultiplier tube detector.³¹ Because of the nitrogen ambient, we are able to measure above the oxygen absorption edge. The measurements were run from 4 to 9 eV (310–138 nm). Because the deuterium lamp has a strong maximum around 170 nm, we were concerned that our low energy results might be affected by scattered light from the strong high energy peak, so we have repeated many of these measurements using various combinations of bandpass and low pass filters. However, we discovered that our concerns were unnecessary; our results showed that these filters had little or no effect on the measurements.

III. RESULTS AND DISCUSSION OF MBD LaScO₃

Within the UV/visible wavelength range, the films are transparent. A Sellmeier model was used for the fit with film thickness as the other parameter. The Sellmeier fit is defined by: $n^2 = A_n + [B_n \lambda^2 / (\lambda^2 - C_n^2)]$, $k=0$; the values we obtain for these parameters are shown in Table I. The index parameter values agree within error bars. For an example of the fit, a comparison of theory and experiment is shown in Fig. 1 for the thick sample. Figure 2 shows the index of refraction for both films.

By extending our energy range we saw both the transparent and absorbing behavior of the MBD LaScO₃ films on Si, and therefore a Sellmeier fit would no longer give an accurate account of the dielectric response. We instead fit the data point-by-point. For the initial analysis, the dielectric response was assumed to be identical to that of single-crystalline LaAlO₃.³¹ The next step was to fix the thickness and let n and k vary from the single-crystalline values to better fit the experimental values. In this way, since we mea-

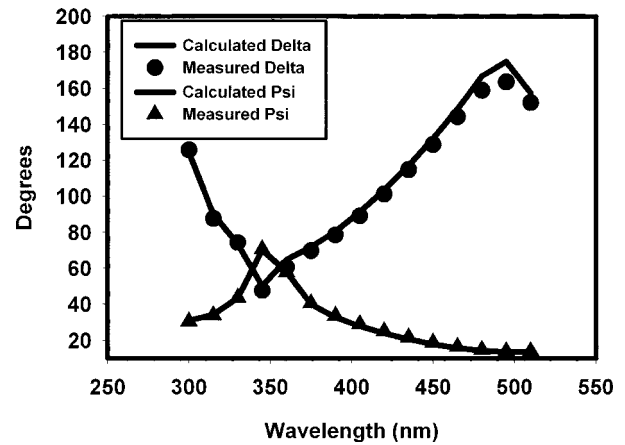


FIG. 1. Calculated (solid) and measured (symbols) ellipsometric parameters for the nominally 100-nm-thick LaScO₃/Si film using a Sellmeier fit for the refractive index.

sured data at N wavelengths, we calculate $2N$ parameters (n and k) from our $2N$ data points [$\tan \psi(\lambda)$ and $\cos \Delta(\lambda)$]. Note that we must fix thickness to avoid having more unknowns than data points. This was done under various assumptions, including a single layer of amorphous LaScO₃ on Si, a mixed interface between the amorphous LaScO₃ and the Si substrate, a SiO₂ interlayer between the amorphous LaScO₃ and the Si substrate, and a reduced density surface layer on the amorphous LaScO₃. By assuming a single layer of amorphous LaScO₃ the comparison between data and simulation is fairly good as seen in Fig. 3. With every point calculated independently, accurate results are shown as a smooth and continuous dielectric constant. An incorrect thickness will result in a discontinuous inferred dielectric response and/or the imposition of critical points of the substrate upon the dielectric response inferred for the overlayer.^{32,33} Such an approach does not force Kramers-Kronig consistent results, however, as would be the case for fitting to some model dielectric function. For the thinner films, this approach worked very well, and we calculated a thickness that is 5 nm less than was inferred by the Sellmeier fit.

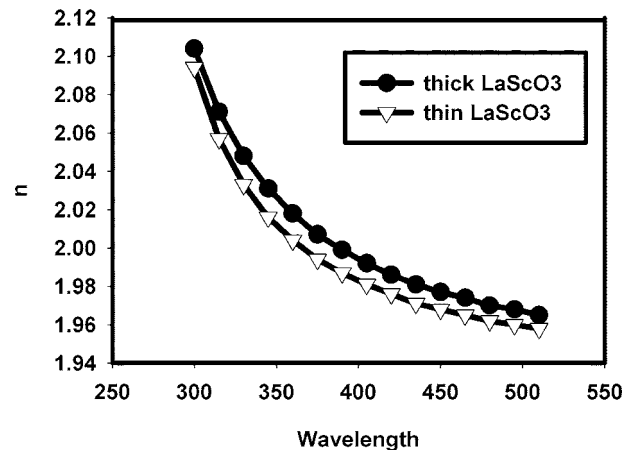


FIG. 2. Best fit refractive index for the nominally 30 nm (∇) and the nominally 100 nm (●) LaScO₃/Si films using a Sellmeier fit.

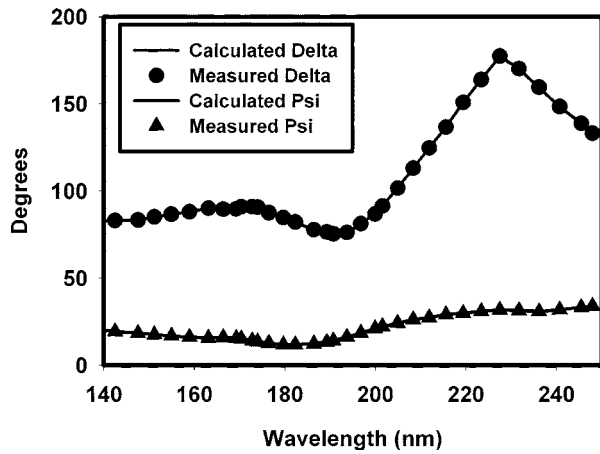


FIG. 3. Measured (solid) and calculated (symbols) ellipsometric angles for the nominally 30 nm LaScO₃ film assuming 34 nm thickness.

The thick film required more than just a single layer model in our analysis of the high photon energy data. To get an adequate result a surface layer of reduced density was added. The layer model was: Si substrate, then an 85-nm-thick full material density layer, and top layer was 40.58 nm thick with a void fraction of 18%. Therefore the total thickness came to 125.6 nm. This differs significantly from the value of 141 nm that the visible spectrum alone gave us.

These two analyses resulted in discrepancies in the thickness for both the thin and thick films. For the thin film there was an 11% difference and for the thick film there was a 13% difference. This may be explained by the fact that the visible spectrum method failed to recognize the second, lower density layer. As defined by its bulk, crystalline density the thin film had a nominal thickness of 30 nm, which is 15% less than what was found. The thick film was predicted by its bulk crystalline density to have a thickness of 100 nm which was again 18% less than what was found.

The next step in our analysis was to determine the band gap. We use the results of these fits to obtain *k* as a function of wavelength, and then calculate alpha ($\alpha = 4\pi k/\lambda$). In Fig.

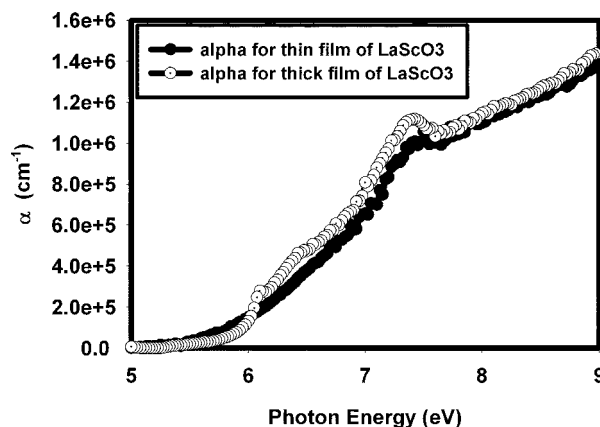


FIG. 4. Absorption coefficient for the nominally 30 nm (●) and the nominally 100 nm (○) thick films of LaScO₃ films on Si.

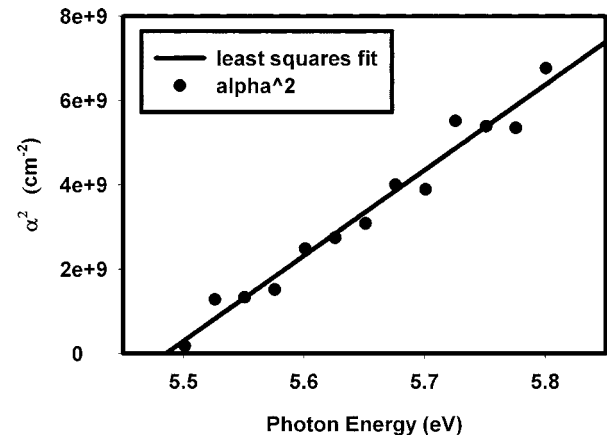


FIG. 5. α^2 (●) vs photon energy for the nominally 30 nm LaScO₃ film. Also plotted is the least squares fit line (solid) leading to $E_G = 5.50$ eV.

4 alpha for both the thin and thick films is shown; notice that for energies under 6 eV the values for the thin film are larger than those for the thick film.

With a direct band gap material, a plot of α^2 vs photon energy should give us a line that intercepts the energy axis at the value of the band gap. The results from the thin film indicate that there are two linear ranges that lead to band gaps of 5.5 and 5.99 eV. With the thick film we only observe a linear region leading to the higher band gap of 5.96 eV. These results imply that the thinner film has the lower band gap of 5.5 eV, and that both the thin and thick films have a strong absorption band gap at around 6 eV. In Fig. 5, α^2 and the linear fit to α^2 for the lower band gap of the thin film is shown. In Fig. 6, the higher band gap for the thin film and the band gap for the thick film are shown.

IV. RESULTS AND DISCUSSION OF PLD LaScO₃

In addition to the films on Si substrates, we also studied both epitaxial and amorphous LaScO₃ films deposited on MgO by pulsed laser deposition.³⁴ Both films were 1.5 μm thick; epitaxial films were deposited on substrates at elevated

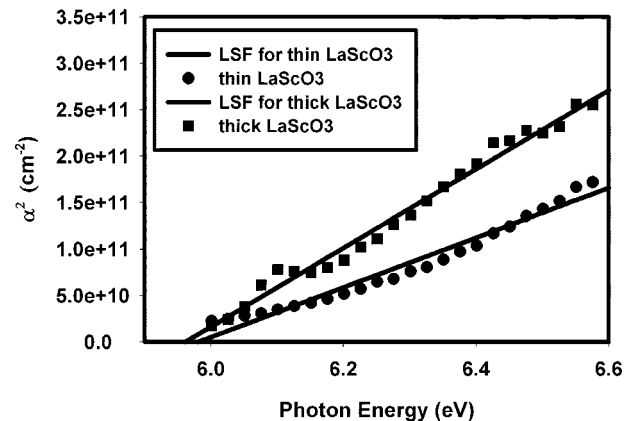


FIG. 6. α^2 vs photon energy for both the nominally 30 nm (●) and the nominally 100 nm (■) LaScO₃ films. Also plotted are the least squares fit lines (solid) leading to $E_G \approx 6$ eV for both films.

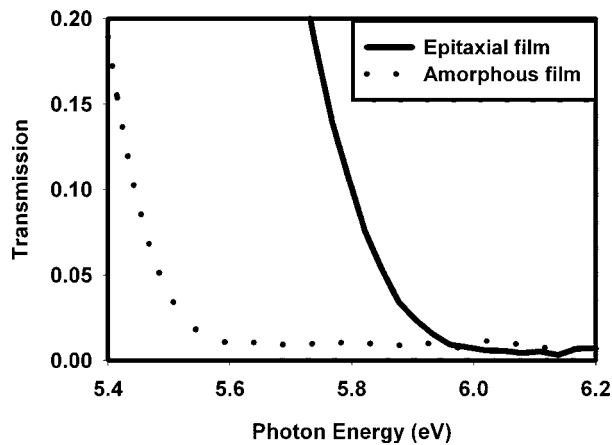


Fig. 7. Transmission spectra of nominally 1.5- μm -thick films of epitaxial (solid) and amorphous (dotted) LaScO_3 deposited upon MgO substrates by pulsed laser deposition.

temperature whereas the amorphous films were deposited on substrates held at room temperature. Transmission of these films was measured from 2 to 6.2 eV. As shown in Fig. 7, the transmission measurements show that the two films have different band gaps. The onset of transmission for the epitaxial film is over 5.8 eV, as compared to the amorphous film that has an onset around 5.5 eV. At this thickness a transmission of 20% implies an absorption coefficient $\alpha \approx 10^4 \text{ cm}^{-1}$, which means the onset of visible transmission occurs in the region of $10^4 < \alpha < 10^5 \text{ cm}^{-1}$.

V. RESULTS AND DISCUSSION OF MBD LaAlO_3

We will now discuss thin films of amorphous LaAlO_3 , which were grown by molecular beam deposition³⁰ on a silicon substrate. The first sample we studied was nominally a 300-nm-thick film of amorphous LaAlO_3 on silicon. The sample was measured on the custom fabricated spectroscopic ellipsometer system described previously.³¹ For the initial analysis, we fit the data point-by-point as described previously in the Sec. IV. The comparison between data and simulation is fairly good as seen in Fig. 8. Using this fit we can again determine the band gap. In Fig. 9 we show a plot of α^2 vs photon energy which indicates a direct band gap of 6.33 eV. This value is in reasonable agreement with Lu *et al.*,³¹ who found a band gap of 6.55 eV for amorphous LaAlO_3 on fused silica.

The final sample we discuss is a 30 nm amorphous LaAlO_3 film on Si. The comparison between model and experiment was fairly good. Again we calculate alpha ($\alpha = 4\pi k/\lambda$) to determine the band gap, and attempt to fit α^2 to a straight line. Using the lower energy points, we attempt to fit a band gap value close to those of bulk LaAlO_3 which is 5.8 eV. We find a good linear fit for a band gap of 5.84 eV. This is substantially less than we found for the thick film.

We investigated further, and added tests for indirect band gaps to our studies. In this case, we sought linear regions for a plot of $\alpha^{1/2}$ vs photon energy. We found a region with a good fit to $\alpha^{1/2}$ for this thin film leading to an inferred indi-

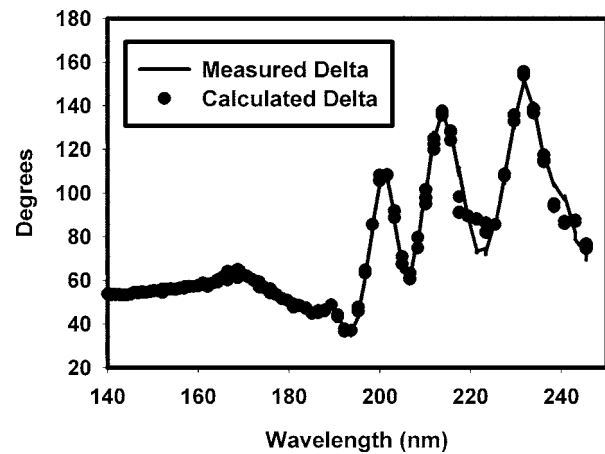


Fig. 8. Comparison between model (●) and data (solid) for the nominally 300-nm-thick LaAlO_3/Si sample.

rect band gap of 5.4 eV. We also found a fit for an indirect band gap of 5.7 eV for the thick film although the standard deviation was twice as great in this case. The absorption coefficient magnitude (in the photon energy range in which we are fitting) is typically over $10\,000 \text{ cm}^{-1}$; this magnitude is similar to that observed for GaAs at 1.5 eV.^{35,36} We note that Kwok and Aita³⁷ observed an indirect band gap in ZrO_2 with similar levels of absorption. Their data were taken by transmission and reflectance spectroscopy.

As shown in Fig. 10, we see differences in α between thin and thick films that are quite similar to those discussed earlier for the LaScO_3 films and illustrated in Fig. 4; in both cases the thinner film exhibits higher absorption at the lowest energies, whereas the thicker films become more absorbing at higher photon energies. We must conclude that the optical response of these films also depends significantly upon the thickness. We note that the scandate films did NOT exhibit indirect band gaps.

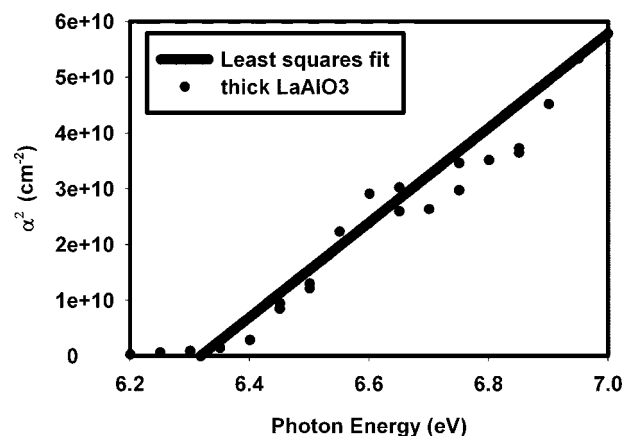


Fig. 9. Least squares fit (solid) to data (●) for the nominally 300-nm-thick LaAlO_3/Si assuming a band gap of 6.33 eV.

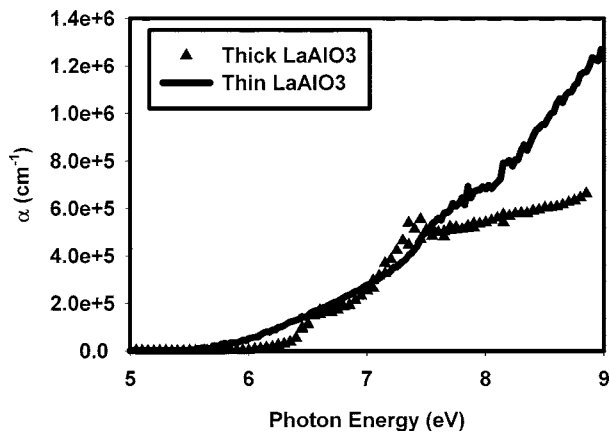


FIG. 10. Absorption coefficient for the nominally 30 nm (solid) and 300 nm (\blacktriangle) thick films of LaAlO₃ films of Si.

ACKNOWLEDGMENTS

E.C. and J.L.F. gratefully acknowledge that this material is based upon work supported by the National Science Foundation under Grant No. 0218288. L.F.E. and D.G.S. gratefully acknowledge the financial support of the Semiconductor Research Corporation (SRC) and SEMATECH through the SRC/SEMATECH FEP Center. L.F.E. gratefully acknowledges an AMD/SRC fellowship. The portion of this work conducted at PNNL was carried out in the Environmental Molecular Sciences Laboratory, a national scientific user facility sponsored by the Department of Energy's Office of Biological and Environmental Research.

This paper was presented at the AVS 51st International Symposium held in Anaheim CA, November 14-19, 2004.

- ¹H. S. Momose, M. Ono, T. Yoshitome, T. Ohguro, S. Nakamura, M. Saito, and H. Iwai, *IEEE Trans. Electron Devices* **43**, 1233 (1996).
- ²D. A. Buchanan and S. H. Lo, presented at the Symposium on the Physics and Chemistry of SiO₂ and the Si-SiO₂ Interface, Los Angeles, 1996.
- ³S. H. Lo, D. A. Buchanan, Y. Taur, and W. Wang, *IEEE Electron Device Lett.* **18**, 209 (1997).
- ⁴M. L. Green, T. W. Sorsch, G. L. Timp, D. A. Muller, D. E. Weir, P. J. Silverman, S. V. Moccio, and Y. O. Kim, *Microelectron. Eng.* **48**, 25 (1999).
- ⁵W. Qi, B. H. Lee, R. Nieh, L. Kang, Y. Joen, K. Onishi, and J. C. Lee, *Proc. SPIE* **3881**, 24 (1999).
- ⁶C. A. Billman, P. H. Tan, K. J. Hubbard, and D. G. Schlom, in *Ultrathin SiO₂ and High-K Materials for ULSI Gate Dielectrics*, edited by H. R. Huff, C. A. Richter, M. L. Green, G. Lucovsky, and T. Hattori (Materials Research Society, Warrendale, 1999), Vol. 567, pp. 409–414.
- ⁷K. J. Hubbard and D. G. Schlom, *J. Mater. Res.* **11**, 2757 (1996).
- ⁸D. G. Schlom, C. A. Billman, J. H. Haeni, J. Lettieri, P. H. Tan, R. R. M. Held, S. Volk, and K. J. Hubbard, *Appl. Phys. A: Mater. Sci. Process.* (to be published).

- ⁹X.-B. Lu, Z.-G. Liu, Y.-P. Wang, Y. Yang, X.-P. Wang, H.-W. Zhou, and B.-Y. Nguyen, *J. Appl. Phys.* **94**, 1229 (2003).
- ¹⁰Y. Zheng, H. Mizuta, Y. Tsuchiya, M. Endo, D. Sato, and S. Oda, *J. Appl. Phys.* **97**, 023527 (2005).
- ¹¹G. Reyna-García, M. García-Hipólito, J. Guzmán-Mendoza, M. Aguilar-Fruti, and C. Falcony, *J. Mater. Sci.: Mater. Electron.* **15**, 439 (2004).
- ¹²X.-B. Lu, Z.-G. Liu, Y. Yang, X.-P. Wang, H.-W. Zhou, and B.-Y. Nguyen, *J. Appl. Phys.* **94**, 1229 (2003).
- ¹³Y. J. Cho, N. V. Nguyen, C. A. Richter, J. R. Ehrstein, B. H. Lee, and J. C. Lee, *Appl. Phys. Lett.* **80**, 1249 (2002).
- ¹⁴J. Leng, S. Li, J. Opsal, D. Aspnes, B. H. Lee, and J. Lee, *Proc. SPIE* **4099**, 228 (2000).
- ¹⁵L. Sun, C. Defranoux, J. L. Stehle, P. Boher, P. Evrard, E. Bellandi, and H. Bender, *Mater. Res. Soc. Symp. Proc.* **786**, 95 (2003).
- ¹⁶R. Liu, S. Zollner, P. Fejes, R. Gregory, S. Lu, K. Reid, D. Gilmer, B.-Y. Nguyen, Z. Yu, R. Droopad, J. Curless, A. Demkov, J. Finder, and K. Eisenbeiser, *Mater. Res. Soc. Symp. Proc.* **670**, K111 (2001).
- ¹⁷W. Vandervorst, B. Bris, H. Bender, O. T. Conard, J. Petry, O. Richard, S. Van Elsocht, A. Delabie, M. Caymax, and S. De Gendt, *Mater. Res. Soc. Symp. Proc.* **745**, 23 (2002).
- ¹⁸S. Logothetidis, P. Patsalaas, E. K. Evangelou, N. Konofaos, I. Tsiaoussis, and N. Frangis, *Mater. Sci. Eng., B* **109**, 69 (2004).
- ¹⁹R. Schmidt-Grund, M. Schubert, B. Rheinländer, D. Fritsch, H. Schmidt, E. M. Kaidashev, M. Lorenz, C. M. Herzinger, and M. Grundmann, *Thin Solid Films* **500–504**, 455 (2004).
- ²⁰P. Boher, P. Evrard, O. Condat, C. Dos Reis, C. Defranoux, J. Ph. Piel, J. L. Stehle, and E. Bellandi, *Thin Solid Films* **798–803**, 455 (2004).
- ²¹A. I. Kingon, J. P. Maria, and S. K. Streiffer, *Nature (London)* **406**, 1032 (2000).
- ²²D. G. Schlom and J. H. Haeni, *MRS Bull.* **27**, 198 (2002).
- ²³B.-E. Park and H. Ishiwara, *Appl. Phys. Lett.* **79**, 806 (2001).
- ²⁴B.-E. Park and H. Ishiwara, *Appl. Phys. Lett.* **82**, 1197 (2003).
- ²⁵S. Stemmer and D. G. Schlom, in *Nano and Giga Challenges in Micro-Electronics*, edited by J. Greer, A. Korkin, and J. Labanowski (Elsevier, Amsterdam, 2003), pp. 129–150.
- ²⁶T. Heeg, J. Schubert, Ch. Buchal, J. L. Freeouf, E. Cicerrella, W. Tian, L. F. Edge, Y. Jia, and D. G. Schlom (unpublished).
- ²⁷Ch. Buchal, L. Beckers, A. Eckau, J. Schubert, and W. Zander, *Mater. Sci. Eng., B* **56**, 234 (1998).
- ²⁸Y. Jia and D. G. Schlom, MRI, Penn State University, University Park, PA.
- ²⁹X. Lu, Z. Liu, Y. Wang, Y. Yang, X. Wang, H. Zhou, and B. Nguyen, *J. Appl. Phys.* **94**, 1229 (2003).
- ³⁰L. F. Edge, D. G. Schlom, S. A. Chambers, E. Cicerrella, J. L. Freeouf, B. Holländer, and J. Schubert, *Appl. Phys. Lett.* **84**, 726 (2004).
- ³¹S.-G. Lim, S. Kriventsov, T. N. Jackson, J. H. Haeni, D. G. Schlom, A. M. Balbashov, R. Uecker, P. Reiche, J. L. Freeouf, and G. Lucovsky, *J. Appl. Phys.* **91**, 4500 (2002).
- ³²H. Arwin and D. E. Aspnes, *Thin Solid Films* **113**, 101 (1984); D. E. Aspnes, A. A. Studna, and E. Kinsbron, *Phys. Rev. B* **29**, 768 (1984).
- ³³U. Rossow and W. Richter, in *Optical Characterization of Epitaxial Semiconductor Layers*, edited by G. Bauer and W. Richter (Springer, Berlin, 1996), pp. 96, 108.
- ³⁴J. Schubert, M. Siegert, M. Fardmanesh, W. Zander, M. Prömpers, Ch. Buchal, J. Lisoni, and C. H. Lei, *Appl. Surf. Sci.* **168**, 208 (2000).
- ³⁵D. E. Aspnes, S. M. Kelso, R. A. Logan, and R. Bhat, *J. Appl. Phys.* **60**, 754 (1986).
- ³⁶D. E. Aspnes and A. A. Studna, *Phys. Rev. B* **27**, 985 (1983).
- ³⁷C. K. Kwok and C. R. Aita, *J. Vac. Sci. Technol. A* **8**, 3345 (1990).